Silicon (2018) 10:257–265
DOI 10.1007/s12633-016-9436-6

ORIGINAL PAPER

Synthesis of Magnetic Fe_3O_4@polyethyleneimine.Mn(II) from Fe_3O_4, [3-(2,3-Epoxypropoxy)propyl]trimethoxysilane, Polyethyleneimine and Mn(II) Acetate as a Novel Silicon-Containing Polymeric Organic-Inorganic Hybrid Nanomaterial and Its Catalytic Investigation Towards the Oxidation of Cyclohexene, Ethyl Benzene and Toluene in the Presence of H_2O_2 as an Oxidant

Roghayeh Tarasi[1] · Ali Ramazani[1] · Massomeh Ghorbanloo[1] · Mehdi Khoobi[2,3] · Hamideh Aghahosseini[1] · Sang Woo Joo[4] · Abbas Shafiee[2]

Received: 28 December 2015 / Accepted: 11 April 2016 / Published online: 13 August 2016

Abstract The surfaces of Fe_3O_4 nanoparticles were modified with [3-(2,3 epoxypropoxy)propyl]trimethoxysilane and polyethylenimine (PEI) and then manganese acetate was loaded on Fe_3O_4@PEI and the resultant Fe_3O_4@PEI.Mn nanoparticles applied as a heterogeneous nanocatalyst. The prepared Fe_3O_4@PEI nanoparticles were characterized by FTIR, powder X-ray diffraction, TGA, VSM, SEM and TEM. The EDAX analysis was used to identify the elemental composition of the prepared Fe_3O_4@PEI.Mn nanoparticles. The catalytic activity and selectivity of the Fe_3O_4@PEI.Mn was examined in cyclohexene, ethyl benzene and toluene oxidation reaction with 30 % aqueous H_2O_2 as an oxidant. Furthermore, the effect of reaction parameters such as kinds of solvents, temperature, oxidant amount and catalyst reusability were investigated. Results show that the original properties of the nanoparticles were well preserved and also good activity and reusability were observed in the oxidation of cyclohexene, ethyl benzene and toluene. Moreover, this heterogeneous catalyst can be recovered with a magnetic field and reused for several times without noticeable loss of catalytic activity.

Keywords Heterogeneous catalyst · [3-(2 · 3 epoxypropoxy)propyl]trimethoxysilane · Magnetic nanoparticles · Oxidation · Polyethyleneimine · Manganese (III) acetate

1 Introduction

Catalysts that provide the best yield of the reaction in reduced temperatures could play an important role in green chemistry. Especially nanocatalysts can provide benefits both of the homogenous and heterogeneous catalysts, including high activity and selectivity and also stability and ease of isolation or recovery, hence they act as a bridge between them.

Among various nanoparticles, magnetite Fe_3O_4 nanoparticles have attracted considerable interest because of their superparamagnetic properties, large surface area to volume ratio, biocompatibility, low toxicity, ease of synthesis and simple modification [1]. Such properties make magnetite Fe_3O_4 nanoparticles, good candidates for various applications, including catalysis [2–5], environmental remediation

✉ Ali Ramazani
aliramazani@gmail.com

✉ Sang Woo Joo
swjoo@yu.ac.kr

[1] Department of Chemistry, University of Zanjan, P. O. Box: 45195-313, Zanjan, Iran

[2] Department of Medicinal Chemistry, Faculty of Pharmacy and Pharmaceutical Sciences Research Center, Tehran University of Medical Sciences, Tehran, 14176, Iran

[3] Medical Biomaterials Research Center, Tehran University of Medical Sciences, Tehran, Iran

[4] School of Mechanical Engineering, Yeungnam University, Gyeongsan, 712-749, Republic of Korea

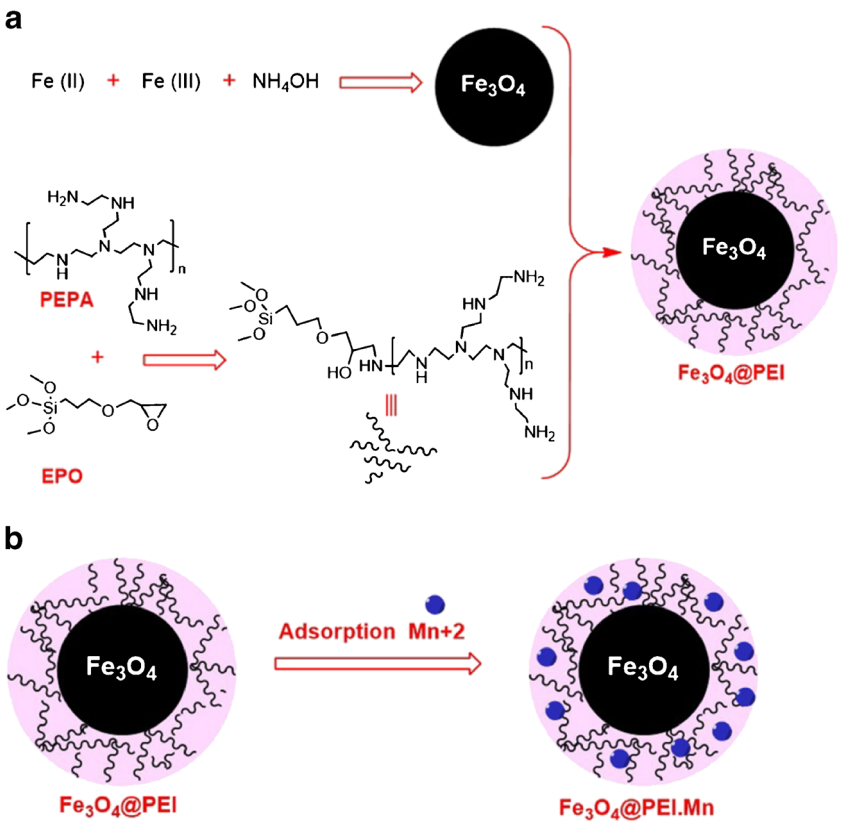

Fig. 1 **a** Schematic representation of the formation of Fe_3O_4@PEI.Mn, PEPA: polyethylenimine, EPO: [3-(2,3-epoxypropoxy)propyl]trimethoxysilane; **b** Mn^{+2} adsorption inside the shell of Fe_3O_4@PEI

[6–8], magnetic resonance imaging (MRI) [9, 10], magneto-thermal therapy [11], magnetic ferro fluids [12], protein purification [13] and drug delivery [14–16].

Recent reports show that application of magnetic nanoparticles as nanocatalysts has attracted much attention because of their advantages such as high catalytic activity, catalyst recovery, higher stability, and easy handling [17–22].

The literature has proposed the synthesis of magnetic nanoparticles with distinct magnetic properties with several methods [23, 24].

Normally, in order to protect and stabilize the magnetic core, as well as retain its magnetic properties, the magnetic core is coated with silica or various polymers [25–27].

Polyethylenimine (PEI) is a cationic polymer with high density of amine functional groups in each polymer chain that possesses a number of advantages, including good

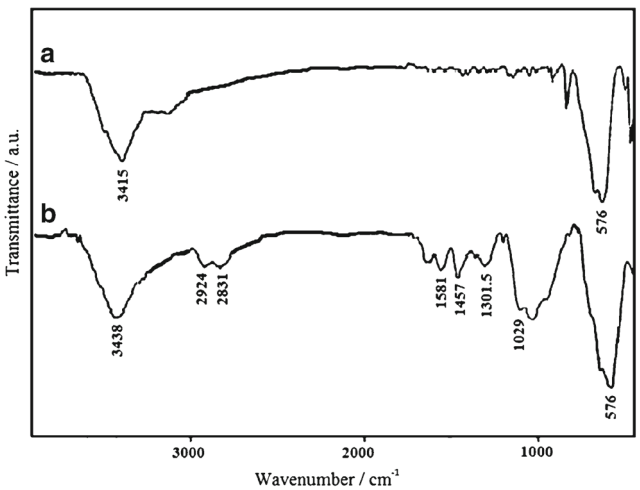

Fig. 2 FTIR spectra of the prepared **a** Fe_3O_4, **b** Fe_3O_4@PEI

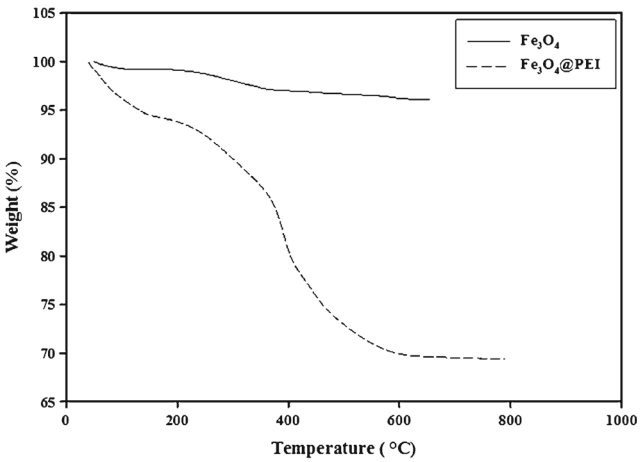

Fig. 3 TGA analysis of Fe_3O_4 and Fe_3O_4@PEI

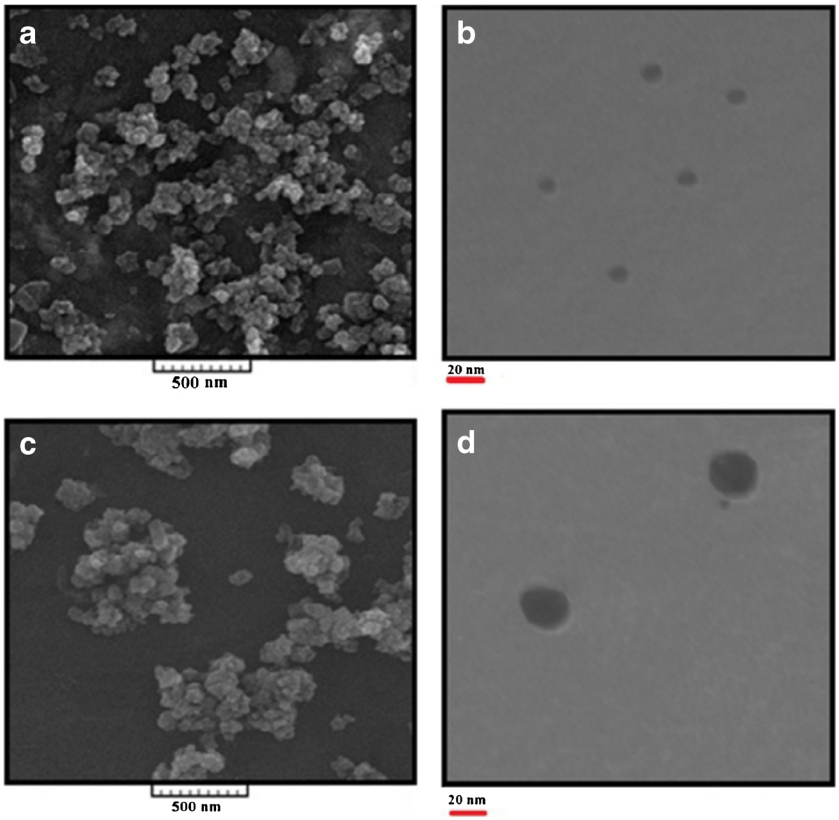

Fig. 4 **a** SEM and **b** TEM images of Fe_3O_4; **c** SEM and TEM **d** images of Fe_3O_4@PEI

water solubility, high content of functional groups, suitable molecular weight, as well as good physical and chemical stabilities [28, 29].

There are several reports about the role of PEI as a shell structure for magnetite nanoparticles [30–32]. Nevertheless, only a few reports could be found about the application of PEI as a catalyst [33–35].

Catalytic oxidation of alkenes is a highly significant chemical reaction in organic synthesis and industrial processes because of the wide usages of epoxides in pharmaceutical industries and as synthetic intermediates in chemical industries [36–38]. Currently, some metal catalysts, such as ruthenium, vanadium, gallium, cobalt, molybdenum and manganese are used for epoxidation of alkenes [39, 40] in the presence of H_2O_2 as an oxidant [41–47]. Hydrogen peroxide (H_2O_2) is a very important oxidant for its environmental cleanness.

This research focuses on preparing a new heterogeneous catalyst via the surface modification of Fe_3O_4 nanoparticles with [3-(2,3 epoxypropoxy)propyl]trimethoxysilane and PEI and the adsorption of manganese acetate on Fe_3O_4@PEI (Fe_3O_4@PEI.Mn). This catalyst was applied successfully in the epoxidation of cyclohexene, ethyl benzene and toluene in the presence of aqueous H_2O_2 (30 %) as an oxidant and it shows high reactivity and selectivity.

2 Results and Discussion

2.1 Preparation of Fe_3O_4@PEI.Mn

In Fig. 1, a schematic representation of the synthesis of Fe_3O_4@PEI.Mn nanoparticles is shown. Interference of silanol groups of EPO with the OH groups of Fe_3O_4, causes the PEI grafting onto the Fe_3O_4.

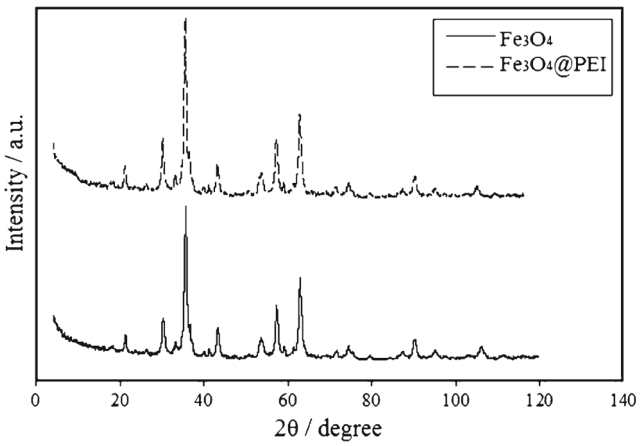

Fig. 5 XRD spectra of the Fe_3O_4 and Fe_3O_4@PEI

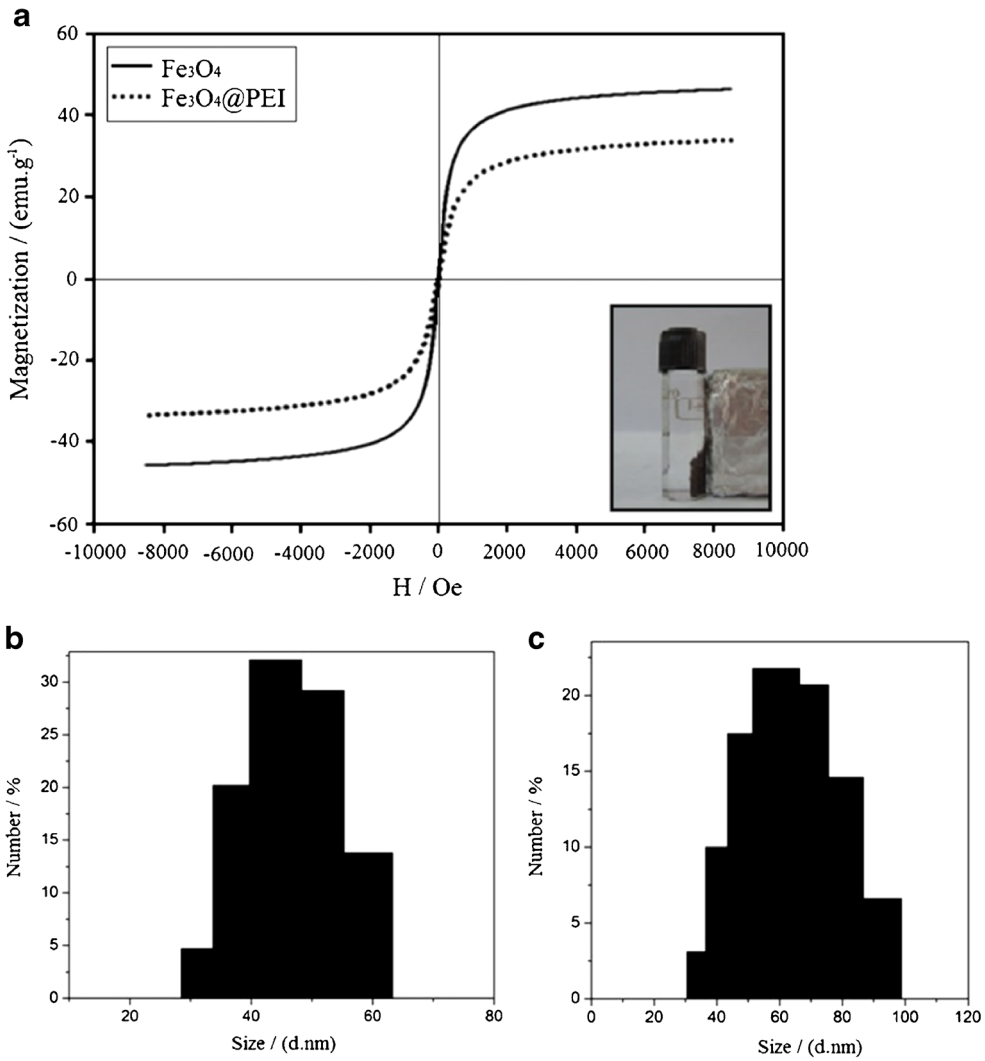

Fig. 6 **a** Magnetization of Fe_3O_4 and Fe_3O_4@PEI. **b** HDs sizes of Fe_3O_4 and **c** Fe_3O_4@PEI

2.2 Characterization of Fe_3O_4@PEI and Fe_3O_4@PEI.Mn

The results of FTIR spectroscopy of the Fe_3O_4 and Fe_3O_4@PEI are shown in Fig. 2a and b, respectively. The characteristic absorption peak of Fe_3O_4 at 576 cm^{-1}, is shown in Fig. 2a. Figure 2b shows the major peaks for Fe_3O_4@PEI as follows: 1110–1000 cm^{-1} (vibration of the Si–O–H and Si–O–Si groups), 584 cm^{-1} (Fe-O stretching vibration), 2924 and 2831 cm^{-1} (C-H stretching vibration), 3415 cm^{-1} (surface-adsorbed water and N-H stretching vibration) and 1457 and 1581 cm^{-1} (C-N stretching vibration).

The TGA analyses of Fe_3O_4 and Fe_3O_4@PEI nanoparticles were carried out over the temperature range of 100 to 800 °C under nitrogen flow and the results are shown in Fig. 3. Figure 3a shows that the weight-loss (4.0 wt%) of iron oxide nanoparticles (Fe_3O_4) in the range of 100 °C to 280 °C, is related to the vaporization of physically and chemically absorbed water. In comparison with Fe_3O_4, the

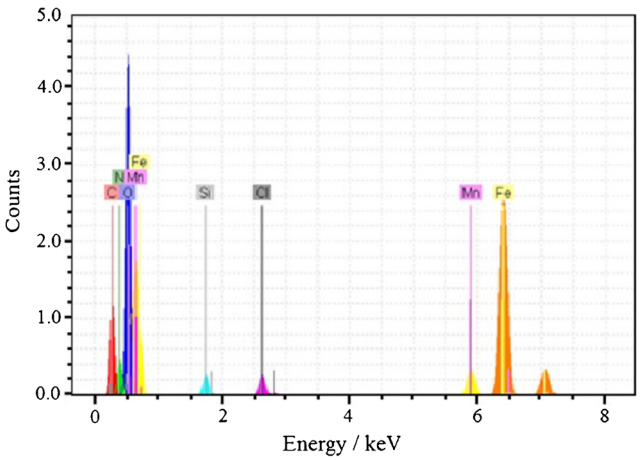

Fig. 7 EDAX spectrum of Fe_3O_4@PEI.Mn catalyst

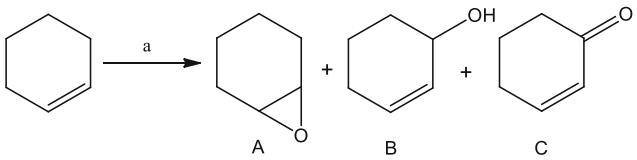

Table 1 Catalytic activity of (Fe_3O_4@PEI.Mn) on cyclohexene oxidation

Entry	$[H_2O_2]$:$[C_6H_{10}]$ (molar ratio)	$NaHCO_3$ [mmol]	Conversion[b] %	Selectivity %		
				A	B	C
1	4:1	0	3	73	27	–
2[c]	4:1	0.5	48	76	24	–
3	6:1	0.5	65	41	43	16
4[d]	8:1	0.5	100	23	31	46

[a]Reaction conditions: catalyst (Fe_3O_4@PEI.Mn) 10 mg; reaction temperature, 60 °C; Cyclohexene, 1 mmol; acetonitrile, 2 ml; reaction time, 4 h;
[b]Conversions are based on the starting substrate;
[c]$NaHCO_3$ (non);
[d]$NaHCO_3$ 0.5 mmol

TGA curve of Fe_3O_4@PEI shows a major decomposition in the temperature range from 400 to 600 °C which indicates the surface grafting of Fe_3O_4 by EPO and PEPA in Fe_3O_4@PEI. The weight loss of EPO and PEPA grafted Fe_3O_4 is 43.1 % (Fig. 3b). The TGA analysis suggests that a moderate degree of PEI modification from the surface of the Fe_3O_4 was successfully achieved.

The SEM and TEM images (Fig. 4) show that the Fe_3O_4 and Fe_3O_4@PEI nanoparticles have approximately spherical shapes and they have average diameters of about 10 and 20 nm respectively.

The X-ray diffraction patterns of Fe_3O_4 and Fe_3O_4@PEI are shown in Fig. 5. The six characteristic peaks at 2θ values of 30.1, 35.4, 43.1, 53.6, 57.1 and 62.7° can be indexed as the diffractions of (2 2 0), (3 1 1), (4 0 0), (4 2 2), (5 1 1) and (4 4 0), respectively. They are similar to the previously reported data for pure Fe_3O_4 nanoparticles with spinel structure [49]. The results indicate that the crystal structure of Fe_3O_4 is not changed after modification with PEI.

The magnetic properties of the Fe_3O_4 and Fe_3O_4@PEI were studied by a VSM at room temperature (Fig. 6a). The specific saturation magnetization (σ_s) for Fe_3O_4 and Fe_3O_4@PEI is 46.4 emu/g and 33.8 emu/g, respectively. Although the presence of PEI weakens the σ_s of Fe_3O_4@PEI, it is still strong enough. The results were also confirmed by the TGA curves. The hydrodynamic diameters of Fe_3O_4 and Fe_3O_4@PEI nanoparticles are in the range of 30–65 nm (Fig. 6b) and 40–100 nm (Fig. 6c), respectively. The hydrodynamic diameter of Fe_3O_4@PEI is greater than for Fe_3O_4. It may result from the higher positively charged surface of PEI in the aqueous dispersion of Fe_3O_4@PEI in comparison with Fe_3O_4.

The C, N, O, Si, Fe and Mn signals can be observed in the EDAX spectrum of the Fe_3O_4@PEI.Mn (Fig. 7).

Table 2 Effect of solvents on the oxidation of cyclohexene catalyzed by (Fe_3O_4@PEI.Mn)

Entry	Solvent	Conversion[a] %	Selectivity[b] %		
			A	B	C
1	MeOH	62	41	21	38
2	CH_3CN	100	23	31	46
3	EtOH	47	32	41	27
4	n-Hexane	0	–	–	–

Reaction conditions: catalyst (Fe_3O_4@PEI.Mn) 10 mg; reaction temperature, 60 °C; cyclohexene, 1 mmol; solvent, 2 ml; $NaHCO_3$ 0.5 mmol; H_2O_2 6 mmol; reaction time, 4 h;
[a]Conversions are based on the starting substrate;
[b]Reaction products (A,B and C) are the same as those in Table 1

Table 3 Effect of temperature on the oxidation of cyclohexene catalyzed by (Fe_3O_4@PEI.Mn)

Entry	Temperature °C	Conversion[a] %	Selectivity[b] %		
			A	B	C
1	40	53	53	41	6
2	60	100	23	31	46
3	80	95	14	25	64

Reaction conditions: catalyst (Fe_3O_4@PEI.Mn) 10 mg; reaction temperature, 60 °C; cyclohexene, 1 mmol; solvent (CH_3CN), 2 mL; $NaHCO_3$ 0.5 mmol; H_2O_2 6 mmol; reaction time, 4 h;

[a]Conversions are based on the starting substrate;

[b]Reaction products (A, B and C) are the same as those in Table 1

These elements are known as the principal elements of the Fe_3O_4@PEI.Mn catalyst.

2.3 Catalytic Activity

The results of control experiments showed that the presence of the catalyst and the oxidant were essential to the oxidation process. The oxidation reaction of cyclohexene did not occur in the absence of H_2O_2, whereas the oxidation reaction without the catalyst continued only up to 6 % after 24 h [50].

When H_2O_2 is used as the sole oxidant, catalytic efficiency of H_2O_2 is rather poor in the presence of catalyst. On the other hand, the cyclohexene oxidation using catalyst/H_2O_2 increased from 1 % to 16 % at 4 h with the addition of a co-catalyst ($NaHCO_3$). This result is related to the poor leaving trend of the hydroxide ion. However, in the presence of sodium bicarbonate, H_2O_2 reacts with bicarbonate in an equilibrium process to produce peroxymonocarbonate (HCO_4^-), which HCO_4^- is a more active nucleophile than H_2O_2 and causes an increase in the rate of the oxidation reaction [51]. When more hydrogen peroxide was used, the conversion increased (Table 1).

To explore the effect of solvent on the reaction, different solvents were used in the same epoxidation reactions and it was observed that the nature of the solvent has a marked effect (Table 2). The highest conversion was observed when the reaction was performed in acetonitrile. The difference is explained by the ready miscibility of acetonitrile with water whereas *n*-hexane is immiscible.

Temperature also was an important factor in the epoxidation reaction, especially in the range of 40 to 60 °C (Table 3), so that when the temperature was elevated from 40 to 60 °C, the conversion increased from 53 % to 100 % but when the temperature increased to 80 °C, the conversion decreased to 95 %. It seems likely that higher temperatures facilitate the decomposition of H_2O_2. As an alternative possibility, at higher temperature, the pH of the reaction increases, because a part of $NaHCO_3$ is converted to Na_2CO_3 and facilitates the higher decomposition of H_2O_2 [52]. This will lead to the reduction of yield (Table 3, entry 3).

Table 4 Effect of oxidant/substrate molar ratio on ethyl benzene oxidation by Fe_3O_4@PEI.Mn

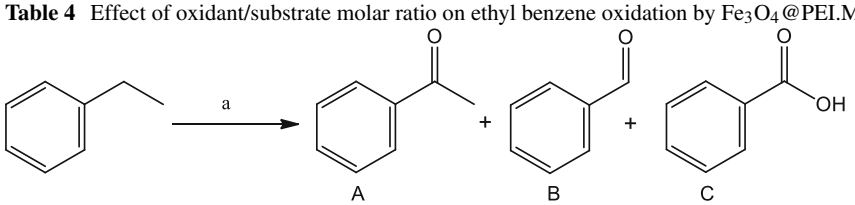

Entry	$[H_2O_2]$:[ethylbenzene] (molar ratio)	Convesion[b] %	Selectivity %		
			A	B	C
1	4:1	14	100	–	–
2	6:1	35	92	6	2
3	8:1	54	81	12	7
4	10:1	50	75	6	19

[a]Reaction conditions: catalyst (Fe_3O_4@PEI.Mn) 10 mg; reaction temperature, 60 °C; ethylbenzene, 1 mmol; solvent (CH_3CN), 2 ml; $NaHCO_3$ 0.5 mmol; H_2O_2; reaction time, 4 h;

[b]Conversions are based on the starting substrate

Table 5 Effect of temperature on ethyl benzene oxidation by Fe_3O_4@PEI.Mn

Entry	Temp °C	Convesion[a] %	Selectivity[b] %		
			A	B	C
1	40	32	100	–	–
2	60	56	81	12	7
3	80	41	71	6	23

Reaction conditions: catalyst (Fe_3O_4@PEI.Mn) 10 mg; ethylbenzene, 1 mmol; solvent (CH_3CN), 2 ml; $NaHCO_3$ 0.5 mmol; H_2O_2 6 mmol; reaction time, 4 h;

[a]Conversions are based on the starting substrate;

[b]Reaction products (A,B and C) are the same as those in Table 4

In order to establish the scope of the activity of (Fe_3O_4@PEI.Mn), the oxidation reactions of toluene and ethyl benzene were also studied, as shown in Table 4. The influence of various reaction parameters such as H_2O_2 concentration (mole of H_2O_2 per mole of ethyl benzene) and temperature were examined to achieve suitable reaction conditions for maximum transformation of ethyl benzene as well as better selectivity for the formation of acetophenone. The effect of H_2O_2 concentration on the ethyl benzene oxidation reaction is presented in Table 4. Acetophenone was formed as the major product, while benzaldehyde and benzoic acid were generated as the other products. Therefore, only the side-chain oxidation was observed.

Four different molar ratios of H_2O_2 to ethylbenzene were used (4:1, 6:1, 8:1, and 10:1 mol) in which the amount of ethylbenzene was kept fixed at 1 mmol in 2 ml of MeCN. When the H_2O_2 to ethylbenzene ratio was increased until the ratio is equal to 8, the conversion of ethylbenzene increased. The catalytic oxidation with 8 mmol of H_2O_2 in 4 h gave 34 % conversion with good selectivity to acetophenone (81 %), (Table 4, entry 3). But in higher ratio than 10:1, the excess amount of H_2O_2 caused the low selectivity to acetophenone (73 %), (Table 4, entry 4). The ethyl benzene conversion and selectivity for acetophenone were decreased when the molar ratio increased up to 4:1. In the presence of an excess amount of H_2O_2, the decrease in the selectivity of acetophenone is due to further oxidation of ethyl benzene.

In addition, the conversion of ethylbenzene and the acetophenone selectivity strongly depended on the temperature in the range of 40 °C to 80 °C. When the reaction temperature increased from 40 °C to 60 °C, The conversion of ethyl benzene also increased (Table 5, Entries 1–2). Generally, by increasing the reaction temperature and time, the conversions grew higher (54 %) and also the reaction selectivity to acetophenone increased (81 %), while the selectivity to benzaldehyde and benzoic acid decreased. Thus, temperature increasing was an effective factor for this oxidation reaction because at low temperature the energy was not sufficient for the activation of H_2O_2 or the catalytic circulation. But the conversion was slightly decreased beyond 60 °C (Table 5, Entry 3). This was possibly caused by acceleration of H_2O_2 decomposition at higher temperature. Also at higher temperature, the selectivity to acetophenone as a main product of ethyl benzene oxidation rapidly declined, while with the temperature rise, the selectivity to other products such as benzaldehyde and benzoic acid increased. As the temperature rose, the acetophenone consumption led to an increase in the amount of benzoic acid [53].

Finally, the oxidation of toluene was studied under the optimized conditions for ethyl benzene oxidation. The oxidation occurs on the side chain of the toluene and resulted in 31 % conversion of toluene with 84 % selectivity for benzaldehyde and 16 % for benzyl alcohol.

In this work, the catalyst and applied method have some advantages such as heterogeneous nature, high reusability, high conversions and selectivity of the catalyst. In addition, the heterogeneous catalyst was easily separated from the reaction mixture and reused at least five times without noticeable loss of activity.

3 Conclusions

Fe_3O_4@PEI.Mn as a silicon-containing catalyst was prepared and characterized and then applied as a catalyst for the oxidation of cyclohexene, ethyl benzene and toluene with 30 % aqueous H_2O_2 as an oxidant. The catalytic activity and selectivity of the Fe_3O_4@PEI.Mn was investigated and the influences of various parameters such as kinds of solvents, oxidant amount, catalyst reusability and temperature have been studied. The results show that the Fe_3O_4@PEI.Mn catalyst is an efficient and robust catalyst, which could be reused for five times without significant loss of activity.

4 Experimental

4.1 Material and Methods

Ferric chloride ($FeCl_3 \cdot 6H_2O$), ferrous chloride ($FeCl_2 \cdot 4H_2O$), ammonia, toluene, ethanol, [3-(2,3-epoxypropoxy)propyl]trimethoxysilane (EPO) and polyethylene polyamine (PEPA, MW= 60,000), were obtained from the Sigma–Aldrich Chemical Company. Other reagents like manganese acetate were purchased from the Merck Chemical Company (Darmstadt, Germany).

4.2 Characterization

FTIR spectra were recorded on Nicolet FT-IR Magna 550 spectrographs with a KBr pellet. X-ray diffraction measurements (XRD) were performed on an XPert MPD advanced diffractometer (Cu (K_α) radiation, λ: 1.5406 Å). Thermogravimetric analysis (TGA, Q50) was performed by heating the sample from room temperature to 800 °C under argon flow at a heating ramp of 10 °C min^{-1}. The morphology of magnetic nanoparticles was investigated with a scanning electron microscope (VEGAII TESCAN) and transmission electron microscope (TEM, EM208 Philips Company). Magnetic properties of the samples were recorded on a vibrating sample magnetometer (VSM, Meghnatis Kavir Kashan Co, Kashan, Iran) at 25 °C. EDAX analysis was recorded by using a Rontec (Germany) electron microscope.

4.3 Preparation of Fe_3O_4 Nanoparticles

The chemical co-precipitation method was used for preparation of magnetic Fe_3O_4 [48]. 1.85 mmol of $FeCl_2.4H_2O$ and 3.7 mmol of $FeCl_3.6H_2O$ were dissolved into 200 ml deionized water at room temperature under vigorous stirring and protected under nitrogen gas. Then 10 ml of ammonium hydroxide (25 %) was dropped into the reaction solution. The mixture was heated to 80 °C for 2 h, and then cooled to room temperature. The products were separated from solution by a magnet and rinsed several times with deionized water and ethanol. Finally, the nanoparticles were dried at 80 °C in a vacuum oven.

4.4 Preparation of Fe_3O_4@PEI and Fe_3O_4@PEI.Mn Nanocomplex

1.5 g of PEPA was dissolved in 200 ml toluene under ultrasonication, then 0.5 ml of [3-(2,3 epoxypropoxy)propyl]trimethoxysilane was added dropwise under stirring at room temperature. The reaction mixture was heated at 100 °C for 24 h under nitrogen atmosphere. After that 2 g Fe_3O_4 was added to the reaction mixture and refluxed at 100 °C for 24 h. The Fe_3O_4 nanoparticles grafted with PEI (Fe_3O_4@PEI) were separated by an external magnet, followed by washing with ethanol three times to replace toluene and drying at 100 °C in vacuum for 24 h. Fe_3O_4@PEI was mixed with manganese acetate as follow: 600 mg manganese (II) acetate was dissolved in 10 ml dry acetonitrile by stirring for 10 min. Then, 800 mg Fe_3O_4@PEI was added to the mixture, sonicated for 30 min and stirred at room temperature for 48 h. Finally, Fe_3O_4@PEI.Mn was purified by an external magnet, washed with ethanol three times, and dried under vacuum for 24 h at 70 °C.

4.5 General Oxidation Procedure

The oxidation of the substrates (cyclohexene, ethyl benzene and toluene) with hydrogen peroxide was carried out in an oil bath in a 25 ml round-bottom flask. In a typical reaction procedure, the substrate (1.0 mmol) along with the solvent (2.0 ml), catalyst (10 mg) and $NaHCO_3$ as co-catalyst were stirred at 60 °C, then the hydrogen peroxide was added. At suitable intervals, aliquots were removed and the reaction products were monitored by gas chromatography by comparing their retention times with those of authentic samples. Yields are based on the added substrate and were determined using a calibration curve. Finally, the catalyst was separated by a magnet.

Acknowledgments This work was supported by the "*University of Zanjan*", "*Tehran University of Medical Sciences*" and "*Iran National Science Foundation: INSF*".

References

1. Ghasemi S, Sadighi A, Heidary M, Bozorgi-Koushalshahi M, Habibi Z, Faramarzi MA (2013) IET Nanobiotechnol 7:100–108
2. Nemati F, Saeedirad R (2013) Chin Chem Lett 24:370–372
3. Maleki A (2012) Tetrahedron 68:7827–7833
4. Yoon TJ, Lee W, Oh YS, Lee JK (2003) New J Chem 27:227–229
5. Kiasat AR, Davarpanah J (2015) Res Chem Intermed 41:2991–3001
6. Elliott DW, Zhang WX (2001) Environ Sci Technol 35:4922–4926
7. Takafuji M, Ide S, Ihara H, Xu Z (2004) Chem Mater 16:1977–1983
8. Guo X, Chen F (2005) Environ Sci Technol 39:6808–6818
9. Byrne SJ, Corr SA, Gun'ko YK, Kelly JM, Brougham DF, Ghosh S (2004) Chem Commun 22:2560–2561
10. Nasongkla N, Bey E, Ren J, Ai H, Khemtong C, Guthi JS, Chin SF, Sherry AD, Boothman DA, Gao J (2006) Nano Lett 6:2427–2430
11. Hiergeist R, Andra W, Buske N, Hergt R, Hilger I, Richter U, Kaiser W (1999) J Magn Magn Mater 201:420–422
12. Hayashi T, Hirono S, Tomita M, Umemura S (1996) Nature 381:772–774
13. Franzreb M, Herzberg MS, Hobley TJ, Thomas ORT (2006) Appl Microbiol Biotechnol 70:505–516
14. Couvreur P, Vauthier C (2006) Pharm Res 23:1417–1450
15. Gupta AK, Curtis AS (2004) J Mater Sci -Mater Med 15:493–496

16. Neuberger T, Schoepf B, Hofmann H, Hofmann M, von Rechenberg B (2005) J Magn Magn Mater 293:483–496
17. Shokouhimehr M, Piao Y, Kim J, Jang Y, Hyeon T (2007) Angew Chem Int Ed 46:7039–7043
18. Polshettiwar V, Varma RS (2010) Green Chem 12:743–754
19. Shylesh S, Schunemann V, Thiel WR (2010) Angew Chem Int Ed 49:3428–3459
20. Lu AH, Salabas EL, Schuth F (2007) Angew Chem Int Ed 46:1222–1244
21. Chikazumi S, Taketomi S, Ukita M, Mizukami M, Miyajima H, Setogawa M, Kurihara Y (1987) J Magn Magn Mater 65:245–251
22. Hu A, Yee GT, Lin W (2005) J Am Chem Soc 127:12486–12487
23. Nikitenko SI, Koltypin Y, Palchik O, Felner I, Xu XN, Gedanken A (2001) Angew Chem Int Ed 40:4447–4449
24. Faraji M, Yamini Y, Rezaee M (2010) J Iran Chem Soc 7:1–37
25. Saeedi MS, Tangestaninejad S, Moghadam M, Mirkhani V, Mohammadpoor-Baltork I, Khosropour AR (2013) Polyhedron 49:158–166
26. Dehghani F, Sardarian AR, Esmaeilpour MJ (2013) Org Chem 743:87–96
27. Zolfigol MA, Khakyzadeh V, Moosavi-Zare AR, Rostami A, Zare A, Iranpoor N, Beyzavi MH, Luque R (2013) Green Chem 15:2132–2140
28. Wilson L, Fernandez-Lorente G, Fernandez-Lafuente R, Illanes A, Guisan JM, Palomo JM (2006) Enzyme Microb Technol 39:750–755
29. Khoobi M, Motevalizadeh SF, Asadgol Z, Forootanfarc H, Shafiee A, Faramarzi MA (2014) Biochem Eng J 88:131–141
30. Loua L, Yua K, Wangb Y, Zhua Z (2012) Appl Surf Sci 258:3744–3749
31. Xiaa T, Guana Y, Yanga M, Xionga W, Wangb N, Zhaoa S, Guob C (2014) Colloids Surf A Physicochem Eng Asp 443:552–559
32. Loua L, Yua K, Zhanga Z, Huanga R, Wangb Y, Zhua Z (2012) Appl Surf Sci 258:8521–8526
33. Veerakumara P, Velayudham M, Lu KL, Rajagopal S (2013) Appl Catal A 455:247–260
34. Shen Z, Chen Y, Frey H, Stiriba SE (2006) Macromolecules 39:2092–2099
35. Wang ML, Jiang TT, Lu Y, Liu HJ, Chen Y (2013) J Mater Chem A 1:5923–5933
36. Weissermel K, Arpe HJ (1996) Industrielle Organische Chemie. Tokyo Kagakudouninn, Tokyo
37. Cui HT, Zhang Y, Qiu ZG, Zhao LF, Zhu YL (2010) Appl Catal B 101:45–53
38. Kooti M, Afshari M (2012) Mater Res Bull 47:3473–3478
39. Lu T, Zhang L, Ge Z, Ji Y, Lu M (2015) Appl Organomet Chem 29:276–279
40. Ruano D, Díaz-García M, Alfayate A, Sánchez-Sánchez M (2015) ChemCatChem 7:674–681
41. Chen S, Liu Z, Shi E, Chen L, Wei W, Li H, Cheng Y, Wan X (2011) Org Lett 13:2274–2277
42. Shringarpure P, Patel A (2010) J Mol Catal A Chem 321:22–26
43. Vafaeezadeh M, Hashemi MM (2013) Chem Eng J 221:254–257
44. Moghadam M, Mirkhani V, Angestaninejad S, Mohammadpoor-Baltork I, Javadi MM (2010) Polyhedron 29:648–654
45. Maurya MR, Kumar A, Pessoa JC (2011) Coord Chem Rev 255:2315–2344
46. Shringarpure PA, Patel A (2011) Chem Eng J 173:612–619
47. Jiang W, Gorden JD, Goldsmith CR (2012) Inorg Chem 51:2725–2727
48. Mu B, Liu P, Dong Y, Lu C, Wu X (2010) J Polym Sci Part A Polym Chem 48:3135–3144
49. Zhou L, Li G, An T, Li Y (2010) Res Chem Intermed 36:277–278
50. Li Y, Fu X, Gong B, Zou X, Tu X, Chen J (2010) J Mol Catal A 322:55–62
51. Maiti SK, Dinda S, Gharah N, Bhattacharyya R (2006) New J Chem 30:479–489
52. Parida KM Soumya-Dash S (2009) J Mol Catal A 306:54–61
53. Li X, Lu B, Sun J, Wang X, Zhao J, Cai Q (2013) Catal Commun 39:115–118